Resting cardiac sympathetic firing frequencies suppress terminal norepinephrine transporter uptake

Cao, Lily; Marshall, Janice; Fabritz, Larissa; Brain, Keith

DOI:
10.1016/j.autneu.2021.102794

Document Version
Peer reviewed version

Citation for published version (Harvard):
Cao, L, Marshall, J, Fabritz, L & Brain, K 2021, 'Resting cardiac sympathetic firing frequencies suppress terminal norepinephrine transporter uptake', *Autonomic Neuroscience*, vol. 232, 102794.
https://doi.org/10.1016/j.autneu.2021.102794

Title: Resting cardiac sympathetic firing frequencies suppress terminal norepinephrine transporter uptake

Authors: Lily L Cao[a], Janice M Marshall[a], Larissa Fabritz[b,c], Keith L Brain[a*]

[a] School of Biomedical Science, Institute of Clinical Science, College of Medical and Dental Sciences, University of Birmingham, UK. B15 2TT

[b] Institute of Cardiovascular Science, College of Medical and Dental Sciences, University of Birmingham, UK. B15 2TT

[c] Department of Cardiology, University Hospitals Birmingham NHS Foundation Trust, Birmingham, United Kingdom

[*] Corresponding author

Emails:

- LLC: LXC319@student.bham.ac.uk
- JMM: janice.m.marshall@bham.ac.uk
- LF: l.fabritz@bham.ac.uk
- KLB: k.l.brain@bham.ac.uk

Corresponding author:

Name: Keith L Brain

Address: School of Biomedical Sciences, Institute of Clinical Science, University of Birmingham, Edgbaston, Birmingham, United Kingdom. B15 2TT

Email: k.l.brain@bham.ac.uk

Abstract

The prejunctional norepinephrine transporter (NET) is responsible for the clearance of released norepinephrine (NE) back into the sympathetic nerve terminal. NET regulation must be tightly controlled as variations could have important implications for neurotransmission. Thus far, the effects of sympathetic neuronal activity on NET function have been unclear. Here, we optically monitor single-terminal cardiac NET activity *ex vivo* in response to a broad range of sympathetic postganglionic action potential (AP) firing frequencies.

Isolated murine left atrial appendages were loaded with a fluorescent NET substrate [Neurotransmitter Transporter Uptake Assay (NTUA)] and imaged with confocal microscopy. Sympathetic APs were induced with electrical field stimulation at 0.2-10 Hz (0.1-0.2 ms pulse width). Exogenous NE was applied during the NTUA uptake- and washout phases to investigate substrate competition and displacement, respectively, on transport.

Single-terminal NET reuptake rate was rapidly suppressed in a frequency-dependent manner with an inhibitory EF_{50} of 0.9 Hz. At 2 Hz, the effect was reversed by the α_2-adrenoceptor antagonist yohimbine (1 μM) ($p<0.01$) with no further effect imposed by the muscarinic receptor antagonist atropine (1 μM). Additionally, high exogenous NE concentrations abolished NET reuptake (1 μM NE; $p<0.0001$) and displaced terminal specific NTUA during washout (1-100 μM NE; $p<0.0001$). We have also identified α_2-adrenoceptor-induced suppression of NET reuptake rate during resting stimulation frequencies, which could oppose the effect of autoinhibition-mediated suppression of exocytosis and thus amplify the effects of sympathetic drive on cardiac function.

Keywords

electrical field stimulation; norepinephrine transporter; left atrium; murine; sympathetic; α_2-adrenoceptors

Abbreviations

NET, norepinephrine transporter

NE, norepinephrine

NTUA, neurotransmitter transporter uptake assay

AP, action potential

EFS, electrical field stimulation

LAA, left atrial appendage

Highlights

- Cardiac single-terminal NET rate is rapidly suppressed by sympathetic nerve activity in a frequency-dependent manner
- At low levels of resting sympathetic activity, NET is suppressed by prejunctional α_2-adrenoceptors
- Substrate competition at the transporter site is likely to contribute to NET suppression at high levels of sympathetic activity

Additional information

- **Data availability statement:** Data available on request from the authors.
- **Competing interests:** None declared.
- **Author contributions:** Experimental concepts and design were devised by LLC and KLB. Data was collected by LLC. LLC analysed the data. LLC, JMM, LF and KLB interpreted the data. Original drafting of the manuscript was performed by LLC and was edited by all authors.
- **Acknowledgements:** We would like thank Dr Andrew Holmes (University of Birmingham) for his critical input and revision of the manuscript.
- **Funding received:** this work was supported by the British Heart Foundation studentship [grant number FS/17/7/32651 to LLC, JMM, LF, KLB] and the British Heart Foundation Accelerator Award [AA/18/2/34218 to ICVS (LF)].

1. Introduction

The Na^+/Cl^--dependent norepinephrine transporter (NET), located on the presynaptic membrane of sympathetic nerve terminals, is responsible for the high-affinity reuptake of released norepinephrine (NE) back into the nerve ending [termed $uptake_1$; Iversen (1963)]. In the periphery, prejunctional NET is crucial for cardiovascular homeostasis as it represents up to 90% of neurotransmitter clearance in the heart (Goldstein *et al.*, 1988, Esler *et al.*, 1990) and is therefore an important determinant of noradrenergic volume transmission. Unsurprisingly, disruptions in NET function are often associated with sympathetic overactivity observed in cardiovascular pathologies such as hypertension, tachycardia, orthostatic intolerance (Schroeder and Jordan, 2012) and heart failure (Kaludercic *et al.*, 2010, Liang *et al.*, 1989).

Many factors influence NET function, including endogenous hormones (Apparsundaram *et al.*, 1998, Mandela and Ordway, 2006b) and psychotropic drugs (Zhou, 2004, Weinshenker and Schroeder, 2007). Governed by kinases and phosphatases, they elicit changes in transporter trafficking, activity and/or expression either independently or in combination (Mandela and Ordway, 2006b). However, the effect of sympathetic nerve activity upon NET in intact tissue preparations remains unclear.

While the increase in NET function induced by membrane depolarisation is well established in *in vitro* systems (Savchenko *et al.*, 2003, Mandela and Ordway, 2006a, Habecker *et al.*, 2006, Sung *et al.*, 2017), the findings *ex/in vivo* remains uncertain. Gillis (1963) demonstrated that, in perfused cat hearts, acute electrical stimulation of sympathetic nerve fibres increased neuronal NE retention in the atria. Corroborated findings were reported later by Chang and Chiueh (1969) in the rat submaxillary gland and Ungerer *et al.* (1996) in the rat heart. Contrastingly, depolarisation has been shown to reduce neuronal NE clearance in the cat spleen (Blakeley and Brown, 1964), guinea-pig vas deferens (Palaić and Panisset, 1969) and rat iris and salivary glands (Häggendal and Malmfors, 1969), with others reporting either no effect (Kirpekar and Wakade, 1968, Yamamoto and Kirpekar, 1972) or were left uncertain (Cervoni and Kirpekar, 1966). In those studies, NET function was assessed by measuring the total uptake of tritiated NE in homogenised tissue or metabolites in the perfusion effluent. However, some tissues also

possess a non-neuronal mode of NE accumulation, termed uptake$_2$, which is well-explored in the rat heart (Iversen, 1965) and present in other tissues and species (Almgren and Jonason, 1974, Major *et al.*, 1978). As the studies of neurone depolarisation on NET generally did not utilise uptake$_2$ inhibitors, observational differences could be explained by the additive effects of uptake$_1$ and uptake$_2$, as well as interspecies/inter-tissue differences in uptake$_2$ kinetics in response to membrane depolarisation (Bönisch *et al.*, 1985). For this reason, it is of particular importance to utilise a technique to study action potential (AP)-evoked NET regulation exclusively at the site of release.

So far, studies of NET function in real-time have been restricted to whole cell patch clamp recordings of transporter-induce currents (Sung *et al.*, 2017), though it would be technically challenging to achieve from axon terminals in intact tissues *ex/in vivo*, particularly in the heart where there is a mixture of peripheral neuronal types as well as the repertoire of non-neuronal cell types (Shivkumar and Ardell, 2016). Recently, we developed a fluorescence-based optical technique that can discern individual noradrenergic terminals in cardiovascular tissue and dynamically monitor their reuptake function *ex vivo* in response to functional manipulations (Cao *et al.*, 2020).

In the current study, we utilise a fluorescent technique to investigate the effects of a broad range of acute sympathetic firing frequencies on single-terminal cardiac NET reuptake rate. Furthermore, we also examined the influences of prejunctional α_2-adrenergic autoreceptors and muscarinic heteroreceptors during nerve stimulation, as well as the contribution of NET substrate competition during uptake and displacement through the transporter.

2. Material and Methods

2.1. Ethics approval

All animal experiments were performed in accordance with the UK Animals (Scientific Procedures) Act 1986 and the ethics guidelines set out by the Animal Welfare and Ethical Review Body (AWERB) at the University of Birmingham. Procedures were performed under an approved UK Home Office license (PPL PFDAAF77F). Animals were housed in individually ventilated cages (n=4 maximum per cage) in the Biomedical Services Unit at the University of Birmingham under standard conditions: 12:12 h light/dark cycle (with light beginning at 0700), 22ºC and 55% humidity. Food and water were available *ad libitum*.

2.2. Animals and tissue isolation

A total of 44 adult male C57BL/6 mice (8-12 weeks, 22-30g; Charles River Laboratories. Margate, UK) were used in this study. Animals were rendered unconscious using deep terminal inhalation anaesthesia (3-5% isoflurane in O_2, flow rate 1.5 mL.min^{-1}) and hearts were rapidly isolated following confirmed negative righting- and pedal reflexes. Hearts were maintained in Krebs-Henseleit buffered (KHB) solution containing (mM): NaCl 118, $NaHCO_3$ 25, KH_2PO_4 1.2, glucose 11, EDTA 0.5, $MgSO_4$ 1.2, $CaCl_2$ 2.5, KCl 4.7 and equilibrated with 95% O_2/5% CO_2, pH 7.4, unless otherwise stated.

2.3. Measurement of NET rate assessed by NTUA

The left atrial appendage (LAA) was dissected free as previously described (Cao *et al.*, 2020), transferred to a Sylgard-lined imaging chamber (2 mL capacity) and securely pinned down as flat as possible. Tissues were continuously superfused at 2 mL.min^{-1} between 35-37ºC with oxygenated KHB for at least 20 min prior to *ex vivo* studies. The imaging chamber was positioned underneath an upright confocal laser scanning microscope (Olympus Fluoview FV1000). To reduce the total number of animals used, the LAA from each animal was cut into two and utilised within 1 h in between; tissues were maintained in gassed KHB and each tissue was used for a different experimental purpose in a randomised order.

The method for determining single-terminal NET reuptake rate was based on our previous description with modification (Cao *et al.*, 2020, Alzahrani *et al.*, 2020). Tissues were initially loaded with a low concentration of fluorescent dye [1:100; Neurotransmitter Transporter Uptake Assay (NTUA); R8173, Molecular Devices, CA, USA] to reveal noradrenergic nerve terminals. NTUA is a substrate for the prejunctionally located NET; as NTUA enters sympathetic nerve terminals the fluorophore becomes unmasked and fluoresces upon entry. An area of sufficient innervation at the resolution of single terminals was identified; following the capture of three control *z*-stacks of 15 slices at 1 µm interval, tissues were subjected to a high concentration of NTUA (1:20) and the increase in intracellular fluorescence was imaged every min. In experiments to explore the effects of drugs on NET reuptake rate, tissues were pre-treated with the drugs of interest prior to and during the 1:20 NTUA test period. The image acquisition software (Olympus Fluoview FV10-ASW, v4.2) was configured to capture 512×512-pixel images on a one-way mode at 2.0 µs/pixel; a water immersion objective lens (40× 0.8 NA, Olympus) was used with wavelength filters set as follows: excitation 405 nm (*circa* 1% laser power); emission 460-560 nm.

2.4. Electrical field stimulation and NET rate

The effect of APs on NET reuptake kinetics was studied with a modification to the NTUA protocol. A custom pair of parallel silver stimulating electrodes was placed on top of the pinned LAA in the imaging chamber to deliver electrical field stimulation (EFS). The tissue was allowed to equilibrate for 20 min. Prior to the superfusion of 1:100 NTUA, the stimulation threshold voltage that reliably elicited cardiomyocyte contraction was empirically determined. In order to monitor noradrenergic terminals in the absence of contraction artefacts, the voltage was reduced by 20% to allow for neuronal depolarisation only. The EFS parameters were based on the greater excitability of neurones compared to cardiac muscle, as demonstrated by the approximate ten-fold briefer chronaxie (Struik, 2017) and the ten-fold lower rheobase (Reilly and Diamant, 2011). The standard NTUA superfusion protocol was then followed through with square-wave pulse stimuli delivered with 1:20 NTUA entry into the imaging chamber (t=0; 0.1-0.2 ms pulse duration) at varying frequencies (0.2, 0.5, 1, 2, 5 and 10 Hz) until the end of the experiment. These frequencies represent the physiological range of resting

and maximal sympathetic activity in the rodent, usually between 0.3-2.4 Hz and 4-8 Hz, respectively (Häbler *et al.*, 1994, Nilsson *et al.*, 1985). Stimuli were delivered by an isolated voltage stimulator (DS2A, Digitimer, Hertfordshire, UK) connected to an optically isolated digital stimulus trigger unit. At the end of the protocol, the stimulation voltage was returned to 100% cardiomyocyte contraction threshold to ensure the intended stimuli were delivered throughout the protocol. In non-stimulating conditions, tissues were exposed to the same electrodes but were not stimulated.

Stimulus-response data were evaluated by sigmoidal curve fitting to median values to yield the inhibitory EF_{50} (EFS frequency inhibiting the half maximal reuptake effect) constrained to a Hill Slope value of 1. Tissues were pre-treated with yohimbine [1 µM, Kazanietz and Enero (1989)] and atropine [1 µM, Nishimaru *et al.* (2000)] for 20 min prior to 2 Hz EFS to assess the prejunctional roles of the α_2-adrenoceptors (α_2AR) and muscarinic acetylcholine heteroreceptors (mAChR), respectively, on NET reuptake rate during EFS.

2.5. Competition of NTUA with exogenous NE at NET

To determine whether NET substrates NE and NTUA would compete or displace each other at the site of the transporter in non-stimulating conditions, exogenous NE was either superfused simultaneously with 1:20 NTUA during the uptake test period [1 µM NE; (Oostendorp and Kaumann, 2000)] or during washout afterwards (0.1-100 µM NE), respectively. Concentration-response data of the latter was evaluated by sigmoidal curve fitting to median values to yield the effective EC_{50} (concentration causing the half maximal washout effect) constrained to a Hill Slope value of 1.

2.6. Analysis of NET reuptake rate of NTUA

Image analysis was performed with Fiji (v1.53c, https://fiji.sc). Following background subtraction of unlabelled areas nearby, the fluorescence of single terminals in the three control *z*-stacks were extracted and averaged (1:100 NTUA; F_{100}) and the fluorescence at all time points of 1:20 NTUA superfusion (t) was noted ($F_{1:20,t}$). The relative NET rate to accumulate NTUA over time was determined by normalising $F_{1:20,t}$ to F_{100} with the

equation below; the linear trendline gradient was expressed as a percentage change over time.

$$\Delta F_{1:20,t} = \frac{F_{1:20,t} - F_{1:100}}{F_{1:100}}$$

Similarly, to investigate the decline in single-terminal fluorescence during washout, the trendline gradient was quantified from the linear decline in fluorescence signal.

2.7. Drugs

The following drugs were used: yohimbine hydrochloride (VWR), atropine sulfate monohydrate (VWR), and (-)norepinephrine (+)-bitartrate salt monohydrate (Sigma). Drugs were dissolved in dH_2O into stock solutions and diluted in KHB to working concentrations on the day of experiment. Control experiments were performed in the presence of drug-free solvents, using identical conditions applied for drug application.

2.8. Statistical analyses

Normality of data was checked with Kolmogorov-Smirnov test. Normally distributed data were expressed as mean±SEM, although data not normally distributed data were expressed as median (Q1, Q3). In data consisting of 2 groups of equal variances, the parametric unpaired *t*-test was used; otherwise the Welch *t*-test was adopted. In data consisting of >2 groups, the non-parametric Kruskal-Wallis test was used, followed by the Dunn's multiple comparison test. A value of $p<0.05$ was deemed statistically significant.

All statistical analyses were carried out on GraphPad Prism (v8, San Diego, USA). Several 'n' abbreviations are used in the text: (i) 'n' is the number of animals and (ii) 'n_t' is the number of individual nerve terminals. Statistical analyses were performed on 'n_t' numbers. On average, each experimental group consisted of 4 animals where 15 nerve terminals were extracted from each animal, totalling the n_t number to 60 per group.

3. Results

3.1. Sympathetic postganglionic APs suppress single-terminal NET reuptake rate

Exposure of the murine LAA to the fluorescent NET substrate, NTUA, revealed networks of fluorescent varicose noradrenergic nerve terminals (Figure 1A). Relative changes in fluorescence during the fluorophore accumulation with time provides a measure of NET reuptake rate (Cao *et al.*, 2020). NTUA was superfused concomitantly with EFS delivery for 6 min (Figure 1B). In the absence of EFS [no stimulation (NS)], the accumulation of terminal-specific fluorescence increased in a linear fashion throughout NTUA exposure (Figure 1B). In the presence of EFS, the NTUA uptake trace became progressively distorted in a frequency-dependent manner, where the initial rise in fluorescence became markedly shallower and thus the normal linearity of uptake was lost (Figure 1B). In the case of 10 Hz stimulation, the NTUA fluorescence fell below the starting fluorescence within 1 min, suggesting not only that uptake was perturbed but also that the initial 1:100 NTUA fluorescence was lost from the terminal. The disruption in NTUA uptake appeared to recover in the last few min of recording. For this reason, NTUA uptake rate was quantified in the first 3 min (termed 'early phase').

Between 0.2-1 Hz EFS, NTUA uptake rate was not perturbed [NS: 16 (8, 23)%.min^{-1}; 0.2 Hz: 14 (9, 22)%.min^{-1} vs. NS: p>0.05; 0.5 Hz: 10 (3, 18)%.min^{-1} vs. NS: p>0.05; 1 Hz: 11 (5, 15)%.min^{-1} vs. NS: p>0.05]. However, NET reuptake rate became significantly reduced at higher AP frequencies - by 63% at 2 Hz [6 (1, 20)%.min^{-1} vs. NS: p<0.01], 69% at 5 Hz [5 (-2, 15)%.min^{-1} vs. NS: p<0.0001] and 75% at 10 Hz [4 (-5, 14)%.min^{-1} vs. NS: p<0.0001] (all EFS groups: n≥4, n_t≥60/group; Kruskal-Wallis test followed by Dunn's multiple comparison; Figure 1C). The inhibitory EF_{50} of the AP-induced suppression of NET rate equated to 0.9 Hz (Figure 1D). Increasing the EFS voltage back to 100% of cardiomyocyte contraction threshold evoked contractions in all experiments, thus confirming consistent delivery of the EFS parameters intended.

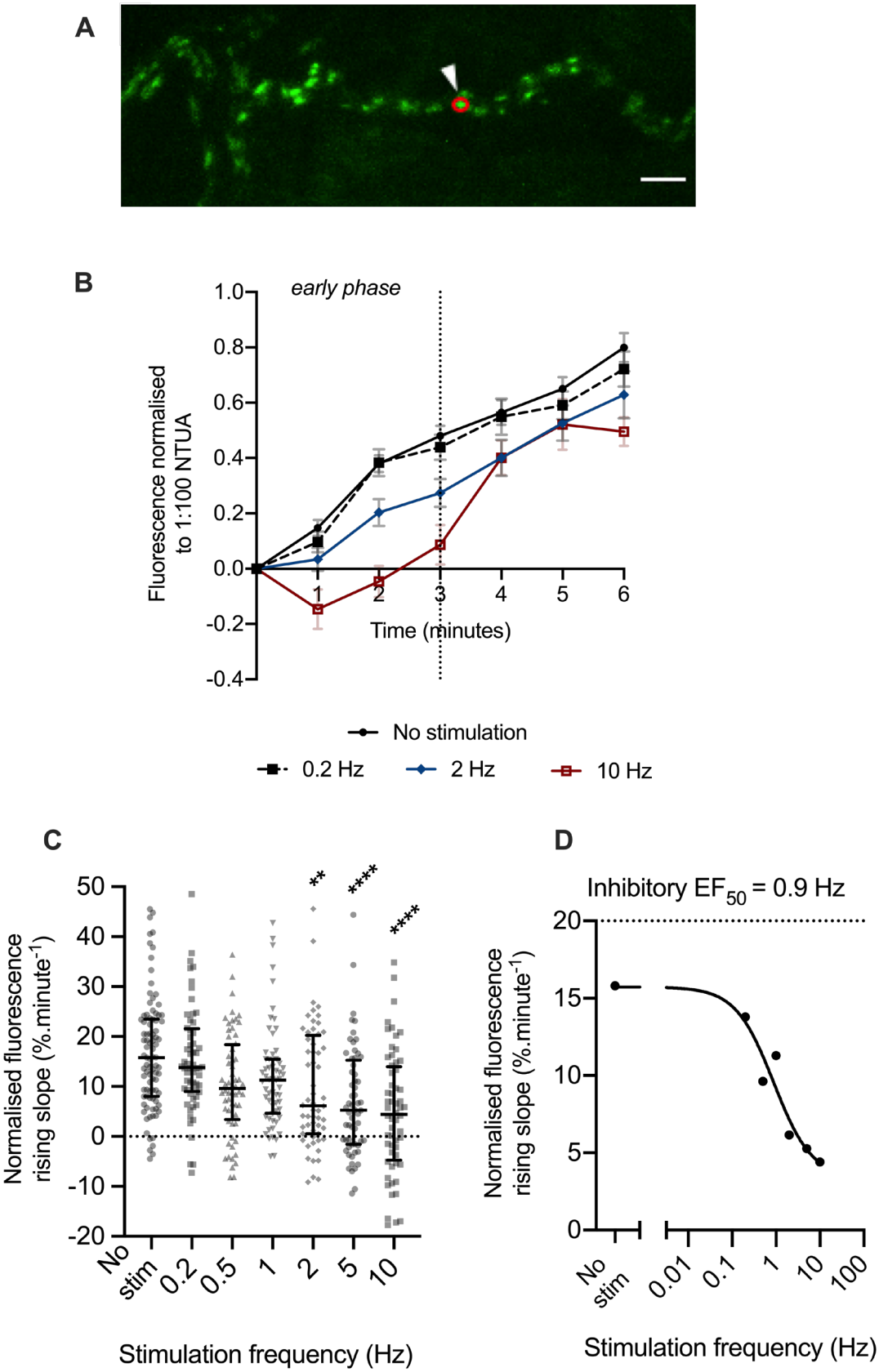
A
B
early phase
Fluorescence normalised to 1:100 NTUA
Time (minutes)
No stimulation
0.2 Hz
2 Hz
10 Hz
C
Normalised fluorescence rising slope (%.minute-1)
Stimulation frequency (Hz)
No stim
D
Inhibitory EF50 = 0.9 Hz
Normalised fluorescence rising slope (%.minute-1)
Stimulation frequency (Hz)
No stim

Figure 1: Cardiac NET reuptake rate is suppressed by sympathetic neurone activity in a frequency-dependent manner.
(A) Representative raw confocal image demonstrating fluorescence of single-terminal cardiac sympathetic nerve fibres labelled with fluorescent NET substrate, NTUA. The uptake of NTUA by single terminals (white arrowhead) was dynamically monitored in response to electrical field stimulation (EFS). Scale bar: 10 μm **(B)** Compared to non-stimulating conditions, the linearity of normalised NTUA accumulation became distorted in response to EFS in the first 3 min. Data presented as mean±SEM. **(C)** NTUA uptake rate was progressively suppressed by EFS in a frequency-dependent manner, where the effect was significant at 2, 5 and 10 Hz. Data presented as median (IQR). Each datapoint corresponds to a single nerve terminal. **(D)** The stimulus-response effect mediated by EFS on NET reuptake rate equated to an inhibitory EF_{50} of 0.9 Hz. Curve fit was conducted on median values previously seen in (C).

** denotes $p<0.01$, **** denotes $p<0.0001$, comparing EFS to 'no stimulation' conditions. Kruskal-Wallis test followed by Dunn's multiple comparison test.

3.2. Role of α_2-adrenoceptors in AP-mediated suppression of NET reuptake rate

To investigate the regulatory role of prejunctional α_2-AR on NET rate during sympathetic neuronal activity, tissues were pre-treated with receptor antagonist, yohimbine (1 μM), for 20 min prior to 2 Hz stimulation. Yohimbine treatment significantly prevented the AP-induced suppression of NET rate during the 'early phase' (2 Hz only: 14±2%.min^{-1} vs. 2 Hz+yohimbine: 20±1%.min^{-1}; p<0.01; n=4, n_t=60/group; Welch's t-test, Figure 2A, B). However, unlike in non-stimulating conditions where NTUA accumulation was linear throughout the 6 min of NTUA exposure, the rise in NTUA fluorescence after yohimbine pre-treatment was only transiently linear in the 'early phase' and became blunted towards a premature plateau by the end of the experiment (Figure 2A).

3.3 Role of muscarinic acetylcholine receptor in EFS-mediated suppression of NET reuptake rate

We previously identified a mAChR-mediated reduction in cardiac NET reuptake rate in non-stimulating conditions (Cao *et al.*, 2020). As our current EFS conditions was likely to have depolarised parasympathetic nerve terminals, we sought to determine whether the evoked release of acetylcholine from local parasympathetic terminals might act upon sympathetic heteroreceptors and affect NET function. Tissues were pre-treated with atropine (1 μM) in addition to yohimbine (1 μM). Blockade of mAChRs did not elicit a further effect on NTUA accumulation compared to yohimbine alone in the 'early phase' [2 Hz+yohimbine: 20±1%.min^{-1} (n=4, n_t=60) vs. 2 Hz+yohimbine+atropine: 19±1%.min^{-1} (n=4, n_t=58), p>0.05; unpaired t-test, Figure 2A, B]. As with α_2AR antagonism, there was a premature plateau of the maximum fluorophore uptake at the end of the 6-min NTUA exposure (Figure 2A).

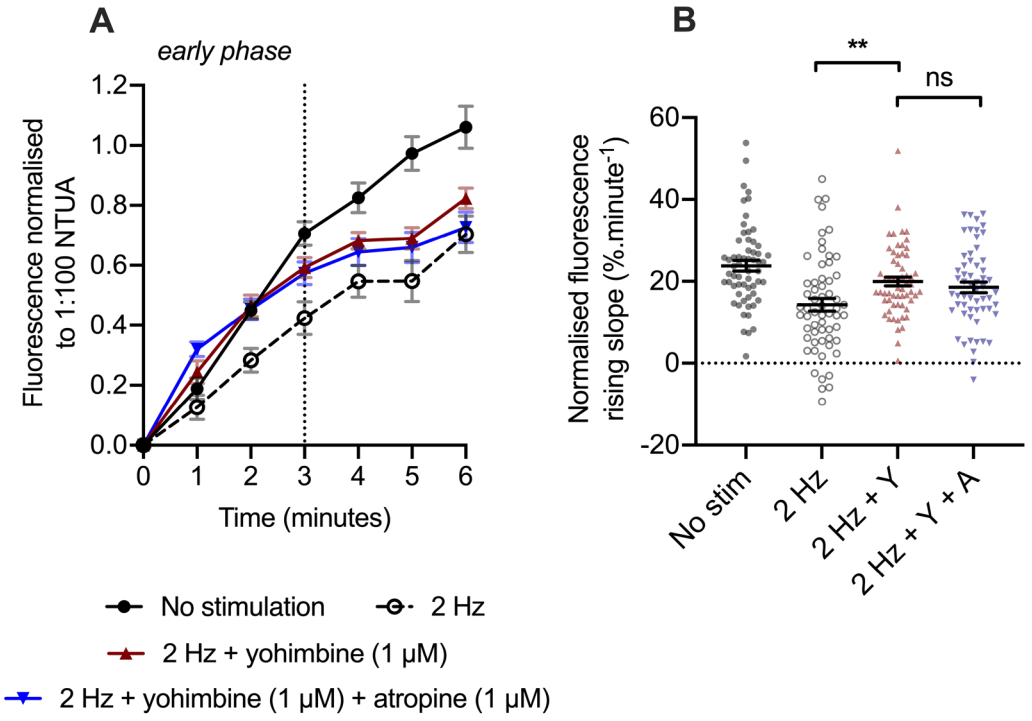

Figure 2: α_2-adrenoceptor inhibition prevents the stimulation-evoked NET suppression
(A) Normalised traces demonstrating NET-mediated NTUA uptake with and without α_2-AR inhibition during EFS (and ± mAChR inhibition). In the presence of yohimbine (Y), the accumulation of NTUA during 2 Hz EFS in the first 3 min recovered, though the maximum accumulation of NTUA thereafter reached a premature plateau. No further effect was mediated by the addition of atropine (Y+A). Data presented as mean±SEM. **(B)** The presence of yohimbine significantly reversed NET rate suppression by 2 Hz EFS, with no further effect by atropine (Y+A). Data presented as mean±SEM. Each datapoint corresponds to a single nerve terminal.

** denotes $p<0.01$ between 2 Hz and 2 Hz+yohimbine; Welch's *t*-test
ns denotes $p>0.05$, comparing 2 Hz+yohimbine with 2 Hz+yohimbine+atropine; unpaired *t*-test

3.4. Exogenous NE competes with NTUA during uptake

If APs were evoked in sympathetic nerve terminals as intended, evoked release of NE could compete with the NTUA fluorophore at the transporter site, thus NE was applied exogenously in non-stimulating conditions to investigate the extent of competition. Simultaneous superfusion of exogenous NE (1 μM) with NTUA prevented fluorophore accumulation into nerve terminals throughout the duration of the experiment (Figure 3A). As a result, exogenous NE completely abolished NTUA uptake rate (control: 10.5±0.7%.min^{-1} vs. NE: -0.4±0.7%.min^{-1}, p<0.0001, unpaired t-test; n=4, n_t=60/group, Figure 3B).

3.5. Exogenous NE displaces NTUA during washout

We also investigated single-terminal NTUA displacement by exogenous NE in a broad concentration range in non-stimulating conditions. Following 1:20 NTUA uptake, tissues were subjected to NTUA washout with KHB ± exogenous NE (0.1-100 μM) (Figure 3C, D). The loss of NTUA fluorescence in the absence of NE occurred at a rate of 7 (-6, 17)%.min^{-1} in the first 2 min. Exogenous NE significantly accentuated the loss by 3-fold at 1 μM [control vs. 1 μM: 25 (17, 45)%.min^{-1}, p<0.0001], 5-fold at 10 μM [control vs. 10 μM: 34 (26, 45)%.min^{-1}, p<0.0001] and 6-fold at 100 μM [control vs. 100 μM: 40 (30-55)%.min^{-1}, p<0.0001], while no effect was observed with 0.1 μM NE [control vs. 0.1 μM: 6 (-1, 14)%.min^{-1}, p>0.05] (n=4, n_t=60/group, Figure 3E; Kruskal-Wallis test followed by Dunn's multiple comparison). The concentration-dependent loss of NTUA fluorescence by exogenous NE equated to an EC_{50} of 0.8 μM (Figure 3F). At very high NE concentrations, the slope of NTUA fluorescence tended towards -1.0 as individual nerve terminals loaded with 1:100 NTUA could no longer be seen (Figure 3C).

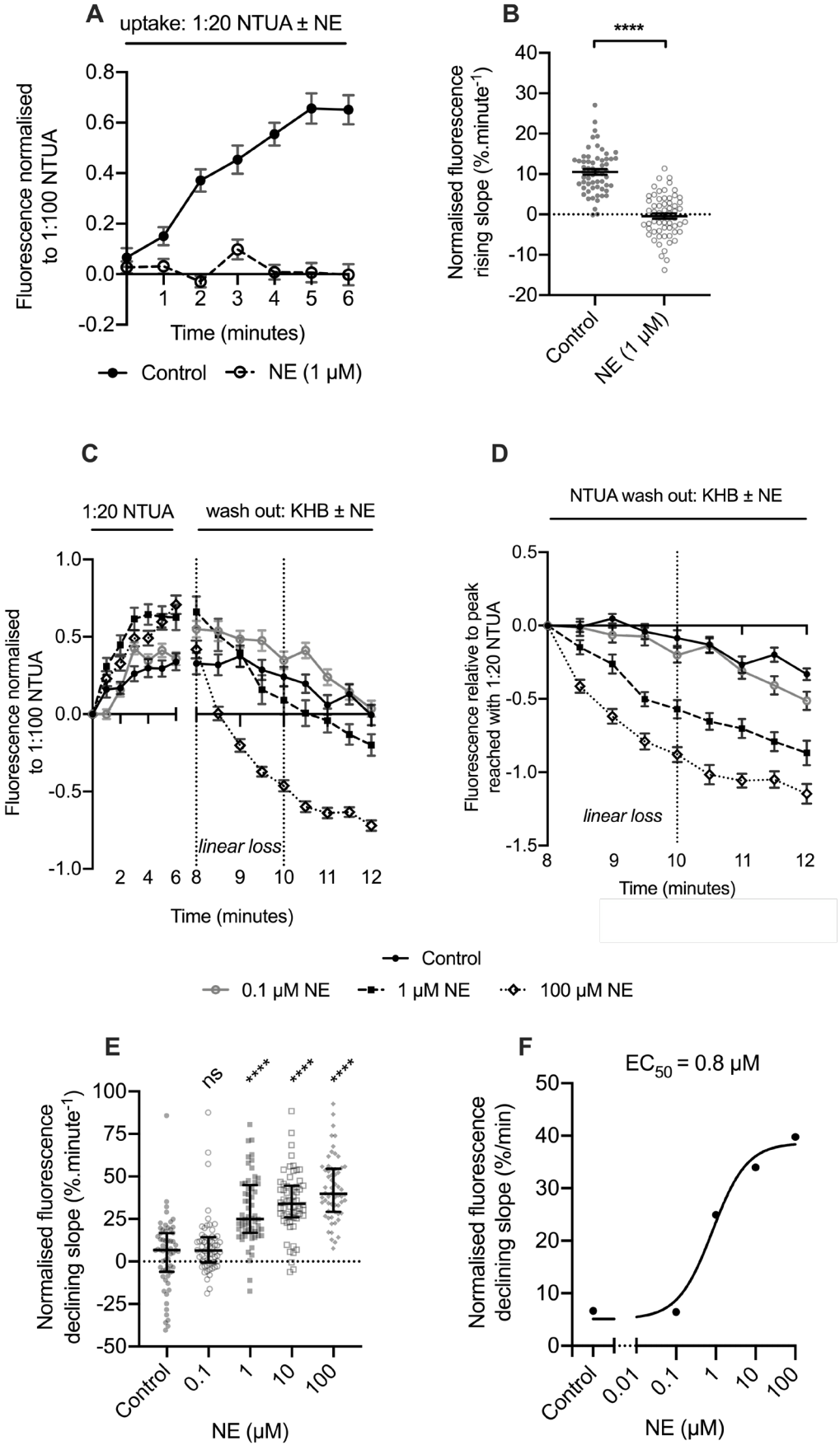
A
uptake: 1:20 NTUA ± NE
Fluorescence normalised to 1:100 NTUA
Time (minutes)
Control
NE (1 µM)
B
****
Normalised fluorescence rising slope (%.minute-1)
Control
NE (1 µM)
C
1:20 NTUA
wash out: KHB ± NE
Fluorescence normalised to 1:100 NTUA
linear loss
Time (minutes)
D
NTUA wash out: KHB ± NE
Fluorescence relative to peak reached with 1:20 NTUA
linear loss
Time (minutes)
Control
0.1 µM NE
1 µM NE
100 µM NE
E
ns
****
****
****
Normalised fluorescence declining slope (%.minute-1)
Control
0.1
1
10
100
NE (µM)
F
EC50 = 0.8 µM
Normalised fluorescence declining slope (%/min)
Control
0.01
0.1
1
10
100
NE (µM)

Figure 3: NET substrate NTUA competition (A-B) and displacement (C-F) with exogenous NE during NET-mediated uptake and washout, respectively,
(A) The accumulation of NTUA into cardiac sympathetic nerve terminals was abolished in the presence of exogenously applied NE (1 μM) at all time points. Data presented as mean±SEM. **(B)** Consequently, the NET-mediated NTUA uptake rate in the presence of NE was significantly reduced, compared to control conditions. Data presented as mean±SEM. **** denotes $p<0.0001$; unpaired *t*-test. Each datapoint corresponds to a single nerve terminal. **(C)** After exposing tissues to NTUA alone, tissues were washed out with KHB±NE (0.1-100 μM). Data presented as mean±SEM. **(D)** NTUA fluorescence was rapidly reduced in the presence of NE in a concentration-dependent manner. Data presented as mean±SEM. **(E)** At NE concentrations ≥1 μM, the loss of NTUA fluorescence was significantly faster than with KHB alone. Data presented as median (Q1, Q3). **** denotes $p<0.0001$ between KHB alone and KHB+NE; Kruskal-Wallis test followed by Dunn's multiple comparison. Each datapoint corresponds to a single nerve terminal. **(F)** The concentration-response effect of NE upon NTUA washout equated to an EC_{50} of 0.8 μM. Curve fit was conducted on median values previously seen in (E).

4. Discussion

4.1. Main findings

We demonstrate here for the first time that acute sympathetic nerve activity at physiological firing rates can rapidly suppresses cardiac NET reuptake rate *ex vivo* at the spatiotemporal resolution of single noradrenergic nerve terminals. By directly measuring for changes in NET rate at the neuroeffector site in intact preparations, the optical technique utilised in this study provides new insight into dynamic mechanisms of transporter regulation and thus sympathetic volume transmission.

We also identify a modulator of NET regulation: the sympathetic prejunctional α_2AR. Acting to rapidly suppress NET rate during sympathetic APs concurrent to a reduction of NE release, the α_2AR may induce a non-linear relationship between resting sympathetic nerve activity and junctional NE concentration. This finding suggests an additional layer of complexity and interconnectedness of multiple mechanisms that can govern release and uptake and reminds us that sympathetic transmission seldomly relies upon the regulation of release alone. Finally, we demonstrate that at high concentrations, NET substrates are likely to compete with and displace each other within the sympathetic nerve terminals, a factor which may have implications for the clinical interpretation of cardiac imaging studies.

4.2. Shortcomings of previous studies

Significant useful information regarding NET function in response to membrane depolarisation has been obtained from *in vitro* systems, where an increase in transporter rate has been observed (Savchenko *et al.*, 2003, Mandela and Ordway, 2006a, Habecker *et al.*, 2006, Sung *et al.*, 2017). However, most studies induced depolarisation with high $[K^+]$ and it may not necessarily reflect transporter function during electrically evoked APs; this is because 1) sustained depolarisation over seconds or minutes does not adequately simulate the millisecond timescale of sympathetic APs, and 2) the activation of protein kinases signalling pathways crucial for NET regulation differs between phasic and chronic depolarising stimuli (Brosenitsch and Katz, 2001). Additionally, *in vitro* methodological settings may limit the translational aspect of transporter regulation in *in* ex*/vivo* systems, where paracrine- and retrograde signalling from other cell types may be

significant (Mandela and Ordway, 2006b, Regehr *et al.*, 2009). Thus, it was pertinent to investigate transporter regulation in intact peripheral end organ preparations.

Interestingly, the observed effects of sympathetic neurone depolarisation on NET function *ex/in vivo* has been unclear in the literature; some reported an accentuation (Gillis, 1963, Chang and Chiueh, 1969, Ungerer *et al.*, 1996), others a depression (Blakeley and Brown, 1964, Palaić and Panisset, 1969, Häggendal and Malmfors, 1969) and some found no effect (Kirpekar and Wakade, 1968, Yamamoto and Kirpekar, 1972). These divergent results could be attributed to the variations in tissue-, species- and methodological choices employed. An example of the latter is stimulation span, whereby acute and chronic depolarisation has been shown to elicit distinct signalling pathways to regulate NET, e.g., transporter membrane translocation and transcription, respectively (Savchenko *et al.*, 2003, Habecker *et al.*, 2006). As depolarising stimuli typically varied between 30 s to 1 h duration, differences in the activated intracellular pathways could add to the inconsistencies in the literature. Finally, traditional *ex/in vivo* studies of neuronal NE clearance often relied on radiochemical or biochemical measurements that often provide results with a significant delay after sample collection (hours to weeks). As the lifetime of NE in a released quantum is estimated to be 5 s (Gonon *et al.*, 1993), improved methods are required to capture the rapid change in transporter kinetics as acute events could be overlooked by end-point studies. Such techniques are available to detect NET kinetics *in vitro* (Sung *et al.*, 2017) and in *ex vivo* models of sympathetic control, e.g. the rat tail artery (Stjärne *et al.*, 1993), although inferences of transporter function in the heart is difficult to achieve due to the mixture of different peripheral neuronal types (Shivkumar and Ardell, 2016).

Here, we utilised a fluorescence-based technique previously developed by our lab (Cao *et al.*, 2020) to dynamically measure NET rate in single postganglionic sympathetic nerve terminals in response to electrically evoked AP propagation *ex vivo*. This optical technique suffices the requirement of high spatiotemporal resolution of single-terminal noradrenergic terminals and provides direct insights into the effect of sympathetic nerve activity on NET regulation. Most importantly, the current study also encompassed a broad range of firing frequencies that is typical of physiological activity - while most studies

utilised those in the maximal range (5-30 Hz), we utilised 0.2-2 Hz, similar to the typical resting states in rodents [about 0.3-2.4 Hz (Häbler *et al.*, 1994)], rising to 5-10 Hz to represent maximal activity [about 6-8 Hz (Nilsson *et al.*, 1985)]. Encompassing a broad range of firing rates in one study should help elucidate NET regulation in states from resting sympathetic tone to hyperactivation.

4.3. Sympathetic postganglionic AP firing suppress cardiac NET kinetics *ex vivo*

In the current study, we demonstrate that EFS-induced sympathetic AP firing rates rapidly suppresses murine cardiac single-terminal NET rate in a frequency-dependent manner. EFS delivered subthreshold for cardiomyocyte contraction (80% cardiomyocyte contraction threshold voltage; 0.1-0.2 ms pulse widths) was sufficient to elicit this effect. This further supports the greater excitability of neurones compared to cardiac muscle, as demonstrated by the approximate ten-fold briefer chronaxie (Struik, 2017) and the ten-fold lower rheobase (Reilly and Diamant, 2011). While we could not confirm AP propagation simultaneously during imaging, we did observe sustained cardiomyocyte contraction in all tissue preparations when the EFS voltage was returned to 100%, thus suggesting EFS was delivered as intended during the protocol.

Our finding differs to the observations of increased NET-mediated inward currents in response to a 2 s depolarising step in single superior cervical ganglion (SCG) neurones (Sung *et al.*, 2017). In addition to the methodological limitations of *in vitro* studies (discussed in 4.2), there is also evidence to suggest functional differences between the sympathetic SCG neurone somata and the nerve terminals in end-organs. Even within the SCG, there are subpopulation differences in AP mechanisms and modulatory responses to NE between sympathetic secretomotor, pilomotor and vasoconstrictor neurones (Li and Horn, 2008). More importantly, 1/3 of SCG neurone somata subpopulations lack the α_2-adreneoceptor-mediated inhibition of sympathetic neuronal excitability (Li and Horn, 2008) and 2/3 lack the expression of co-transmitter neuropeptide Y (NPY) (Gibbins, 1991). As these features are important well-established functional phenotypes of peripheral sympathetic postganglionic terminals in the heart (Wehrwein *et al.*, 2016), and that the (to our knowledge) *in vitro* SCG studies of NET function did not distinguish between neuronal types, we believe such findings cannot be extrapolated with certainty

beyond *in vitro* systems. Our finding also differs with work by Shanks and colleagues (2013a), where there appeared to be a stimulation-evoked increase in NET function in rat sympathetic (cardiac) stellate ganglion neurone somata (though statistical significance was not reported). However, the NE metabolite dihydroxyphenylglycol (DHPG) is absent in the rat stellate ganglia (Bayles *et al.*, 2019), which may imply that NET uptake and metabolism of NE may differ between somatic-dendritic sites and terminals. Regardless, it is also possible the differences in the effect of EFS upon NET between the mouse (current study) and the rat [if present; Shanks *et al.* (2013a)] is also due to species differences in sympathetic transmission. So, while previous work on ganglia provides important functional implications for synaptic integration and ganglionic physiology; here we add new insight into AP-evoked modulation of neurotransmitter clearance at the end-organ where junctional NE availability determines the extent of neuromodulation.

4.4. α_2-Adrenoceptor: a regulator of NET kinetics?

The α_2-AR are powerful autoreceptors that allow NE to inhibit its own release during neuronal activity (Starke, 2001), though its effect on neuronal clearance in the heart is unknown. In the rat locus coeruleus slices, α_2-AR does not affect NET (Callado and Stamford, 2000), though transporter regulation by NE autoreceptors may well be different in the peripheral nervous system. What is known, however, is that the activation of $G_{q/11}$- and $G_{i/o}$-coupled mAChRs on sympathetic nerve terminals can not only reduce neuronal excitability for autonomic cross-inhibition (Trendelenburg *et al.*, 2003, Yang *et al.*, 2006), they can also suppress NET rate (Parker *et al.*, 2010, Cao *et al.*, 2020). Thus, it is possible that other $G_{q/11}$- or $G_{i/o}$-protein coupled receptors, α_2AR being an example of the latter, can also regulate NET. This hypothesis was supported with the finding of an early reversal of EFS-mediated NET suppression by the α_2AR antagonist yohimbine. 2 Hz was chosen because, even though the inhibitory EF_{50} of the stimulus-response effect on NET was 0.9 Hz, the effect on NET function at 1 Hz was not significant.

Although NET is regulated by a plethora of protein kinase and phosphatases (Mandela and Ordway, 2006b), it is not clear by which mechanism(s) the $G_{i/o}$-protein coupled α_2AR acts to reduce NET function. It may be that the main $G_{i/o}$ secondary messengers, cyclic AMP and protein kinase A, exerts a direct effect on NET, though its manipulations in

either direction have produced contrasting observations in a strongly cell line- and species-dependent manner (Mandela and Ordway, 2006b). An alternative mechanism is via the $G_{\beta\gamma}$ complex, which inhibits N-type calcium channel open probability to reduce neuronal excitability [review: Starke (2001)]. The reduction in intracellular Ca^{2+} would in return lower the activities of Ca^{2+}-dependent kinases that can modify NET regulation. Ca^{2+}/calmodulin-dependent kinases (CaMK) and p38 mitogen activated kinases are possible candidates for the effect observed, as activation of these kinases has been shown to increase NET surface trafficking (Apparsundaram *et al.*, 2001, Sung *et al.*, 2017) (Figure 4). For example, the N-terminus of NET can be directly phosphorylated at threonine 30 by CaMKs to alter its surface expression (Sung *et al.*, 2017). Thus, it is possible its inactivation in the absence of Ca^{2+} would attenuate transporter function. However, we did not explore the exact downstream intracellular pathways activated by α_2AR to reduce NET rate, thus it would warrant further investigation to elucidate the pathways for the effect observed.

4.5. Physiological relevance of α_2-adrenoceptor-mediated NET inhibition

There are a host of regulatory mechansism for sympathetic junctional transmission, including feedback mechanisms mediated by NPY and other co-transmitters [for review, see Burnstock (2013)], but amongst these the α_2AR-mediated pathways are central (Stjärne, 1989). The α_2-AR is an important suppressor of NE release and their dysfunctions are often associated with sympathetic overactivity (Gilsbach and Hein, 2012), thus one would query the its functional role to reduce NET suppression during AP propagation. We suggest that α_2-AR would be important mediators to modulate and maintain appropriate junctional NE concentrations crucial for cardiac function. At low resting sympathetic nerve activity, single quanta are released randomly at very low probability, about 0.002-0.02 per varicosity (Åstrand and Stjärne, 1989), with highly efficient junctional clearance to ensure that low levels of activity are virtually ignored (Stjärne *et al.*, 1993, Stjärne *et al.*, 1994). However, at very high frequencies where release probability increases due to frequency facilitation [a form of short-term junctional potentiation (Brain and Bennett, 1997)], junctional NE clearance consequently becomes saturated (Stjärne *et al.*, 1993, Stjärne and Stjärne, 1995) which can lead to a non-linear relationship between sympathetic nerve activity and junctional NE concentration. This

was demonstrated through the use of amperometry in the rat tail artery by Stjärne and colleagues (1993, 1995). In the current study, we demonstrate that even before transporter saturation occurs, prejunctional α_2AR could suppress NET transporter rate, bringing the occurrence of non-linearity within the physiological range of sympathetic activity. This increase in junctional gain at physiological AP firing frequencies would in return increase the metabolic efficiency of junctional neurotransmission (Figure 4); by transiently suppressing uptake, fewer quanta are needed sustain sympathetic cardiac modulation. We recognise the α_2AR antagonist, yohimbine, was not able to completely reverse the effects of nerve stimulation on transporter function (Figure 2A); however, this could be explained by the fact that another mechanism, presumably substrate competition (section 4.7), prevails to influence transporter kinetics during longer trains of stimuli.

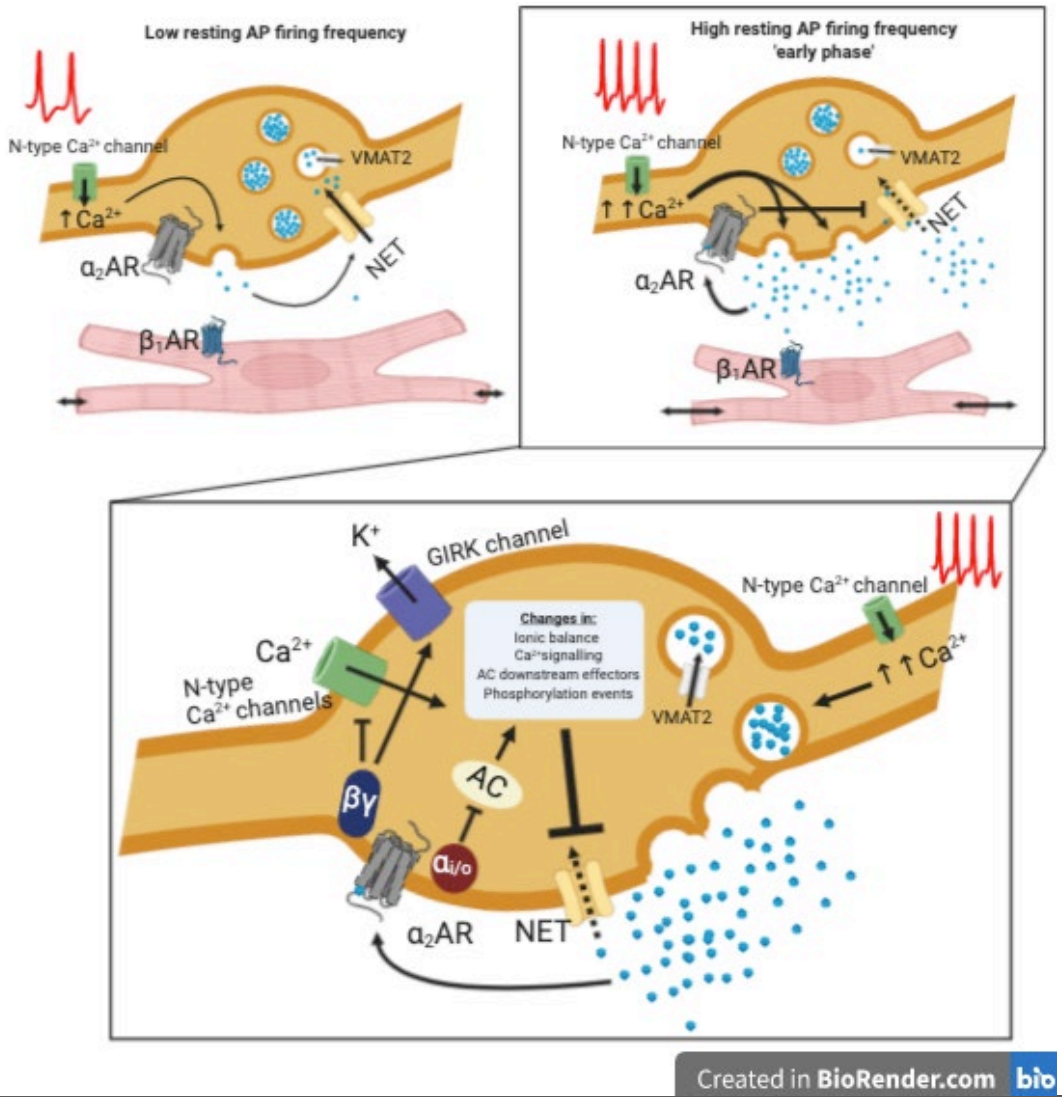

Figure 4: Schematic diagram of α_2-adrenoceptor (α_2-AR)-mediated NET rate suppression during resting sympathetic neuronal activity
(A) At low resting sympathetic activity, single quanta of NE are released at very low probability, and the efficient clearance by NET means that low levels of activity are virtually ignored. **(B)** At high resting sympathetic firing frequencies where NE release is high, but before NET saturation occurs, the α_2-AR can suppress NET rate thus producing a non-linear relationship between neuronal activity and junctional NE availability. **(C)** α_2-AR-mediated NET rate suppression could occur via several mechanisms (but not restricted to): downstream effects of G_α-mediated inhibition of AC, $G_{\beta\gamma}$-mediated inhibition of N-type Ca^{2+} channels and activation of GIRK. However, this prompts further investigation.

Schematic was adapted with concepts from the following sources: Stjärne and colleagues (1993, 1994), Mandela and Ordway (2006b) and this current study.

Abbreviations: action potential, AP; α_2-adrenoceptor, α_2AR; norepinephrine transporter, NET; β_1-adrenoceptor, β_1AR; G-protein coupled inwardly rectifying potassium channel, GIRK; vesicular monoamine transporter 2, VMAT2.

4.6. No mAChR-mediated effect on NET during sympathetic AP propagation

It is likely our stimulating conditions also depolarised parasympathetic nerve terminals in the heart. However, while we previously demonstrated a mAChR-mediated reduction in NET reuptake rate with an exogenous agonist in the vas deferens and the heart (Parker *et al.*, 2010, Cao *et al.*, 2020), the current EFS conditions showed no evidence for autonomic interactions from parasympathetic to sympathetic nerve terminals, a possible explanation being very high endogenous concentrations of ACh achieved at ≥2 Hz are required to suppress the transporter.

4.7. Substrate competition at NET

NE released by EFS is likely to compete with the NTUA fluorophore for transport; our results with exogenously applied NE supports this. Firstly, we show a complete abolition of NET rate with exogenous NE (1 μM) at a concentration that maximally increases rodent left atrial tension [pEC_{50}: 6.8 (Oostendorp and Kaumann, 2000)]. Furthermore, exogenous NE only displaced NTUA at concentrations close to 1 μM (EC_{50}: 0.8 μM), while no effect was observed at NE concentrations ten-fold lower (0.1 μM) (Figure 3E). Additionally, when the inhibition of α_2AR was maintained after the initial 'early phase' of NET uptake (and hence NE release probability was high), the transporter-mediated uptake of the NTUA approached a premature plateau (Figure 2A) where the peak accumulation of the fluorophore was poor. This suggests the gradual increase in junctional NE attributed to α_2AR inhibition during EFS ultimately led to sufficient NE concentrations to compete with the fluorophore at the transporter site. Together, these findings imply that, while α_2AR initially mediates NET suppression during fluctuations in physiological firing frequencies, substrate competition comes to dominate suppression after several minutes of sustained stimulation (at least at 2 Hz when exocytosis is high in the presence of yohimbine), and at higher frequency stimulation frequencies (Stjärne *et al.*, 1993, 1994).

4.8. Clinical implications of NET suppression

Hypertension, at least in spontaneously hypertensive rats (SHRs), can be experimentally induced by either a loss of α_2AR-mediated negative feedback (Zugck *et al.*, 2003) or NET impairment (Shanks *et al.*, 2013a, Shanks *et al.*, 2013b), thus implying that changes in

both α_2AR and NET function are clinically important for hypertension. Hence, it would be very interesting to determine whether the α_2AR-NET coupling we demonstrate here in the healthy rodent is altered during the pathogenesis in SHRs.

We also postulate that cardiac clinical imaging studies involving NET tracer substrates, such as [^{123}I]-metaiodobenzylguanidine (^{123}I-MIBG), under high sympathetic tone may be affected by both the α_2AR-mediated NET inhibition and substrate competition. Interestingly, decreased NET tracer uptake is often observed in patients with noradrenergic overactivation, such as myocardial infarction and stress-induced cardiomyopathies (Schroeder and Jordan, 2012). What is often unknown, however, is whether these patients have reduced NET expression (due to terminal loss) or whether NET transporter activity had been transiently suppressed by the mechanisms we have described. Our findings suggest that NET inhibition or substrate competition under high sympathetic tone could inhibit ^{123}I-MIBG uptake, and so confounding the interpretation of clinical imaging studies.

4.9 Limitations

In our study, we are aware of the great variability of single-terminal NET reuptake rate, where NET function appears suppressed in some terminals but not in others. Furthermore, this variation increases in a frequency-dependent manner such that the range of NET reuptake rates doubles at 10 Hz compared to non-stimulating conditions (Figure 1C). This could be explained by the low intrinsic probability of neurotransmitter release in response to neuronal depolarisation (Brain *et al.*, 2002), meaning that not every nerve terminal stimulus would result in the stimulus-secretion coupling, despite no failure of AP propagation. Alternatively, it may be that some sympathetic terminals fail to respond to EFS under the stimulus conditions used, a feature incidentally noted during experiments in Ca^{2+}-indicator-loaded terminals in the vas deferens (Brain and Bennett, 1997).

Another limitation of the current study is whether the EFS conditions *ex vivo* truly represents resting and maximal sympathetic nerve activity *in vivo*. Here, EFS was held constant throughout NTUA exposure to measure NET reuptake rate. We suggest that, while compound APs of sympathetic nerve activity show asynchronous firing of neurones

that appear in bursts (Nilsson *et al.*, 1985), single fibre analysis show that individual axons rarely fire doublets (Rook *et al.*, 2014). Hence, EFS at a regular frequency to some extent replicates the synchronous activation of noradrenergic terminals (driven by the cardiac cycle), with predominately singlet firing at the level of individual axons (where imaging resides).

5. Conclusion

In summary, this study utilised an optical fluorescence-based technique to detect for a frequency-dependent suppression of NET reuptake rate during physiological sympathetic firing activity. Using this technique, we overcome the methodological limitations associated with previous studies of membrane depolarisation and NET, which provide new insights into the regulation of transporter function at the site of release. We also uncover a role for the prejunctional α_2AR to suppress NE clearance during neuronal activity, which may evoke a non-linear relationship between resting sympathetic nerve activity and junctional NE concentration. Finally, we propose reasons for the reconsideration of clinical imaging interpretations with NET tracer substrates.

References

Almgren, O. & Jonason, J. (1974) Functional significance of neuronal and extraneuronal transmitter uptake in rat salivary glands. *Naunyn Schmiedebergs Arch Pharmacol,* **283,** 1-20.

Alzahrani, A. A., Cao, L. L., Aldossary, H. S., Nathanael, D., Fu, J., Ray, C. J., . . . Holmes, A. P. (2020) β-Adrenoceptor blockade prevents carotid body hyperactivity and elevated vascular sympathetic nerve density induced by chronic intermittent hypoxia. *Pflugers Arch,* **473,** 37-51.

Apparsundaram, S., Galli, A., DeFelice, L. J., Hartzell, H. C. & Blakely, R. D. (1998) Acute regulation of norepinephrine transport: I. protein kinase C-linked muscarinic receptors influence transport capacity and transporter density in SK-N-SH cells. *J Pharmacol Exp Ther,* **287,** 733-43.

Apparsundaram, S., Sung, U., Price, R. D. & Blakely, R. D. (2001) Trafficking-dependent and -independent pathways of neurotransmitter transporter regulation differentially involving p38 mitogen-activated protein kinase revealed in studies of insulin modulation of norepinephrine transport in SK-N-SH cells. *J Pharmacol Exp Ther,* **299,** 666-77.

Åstrand, P. & Stjärne, L. (1989) On the secretory activity of single varicosities in the sympathetic nerves innervating the rat tail artery. *J Physiol,* **409,** 207-20.

Bayles, R. G., Tran, J., Olivas, A., Woodward, W. R., Fei, S. S., Gao, L. & Habecker, B. A. (2019) Sex differences in sympathetic gene expression and cardiac neurochemistry in Wistar Kyoto rats. *PLoS One,* **14,** e0218133.

Blakeley, A. G. H. & Brown, G. L. The effect of nerve stimulation on the uptake of infused noradrenaline by the perfused spleen, In: Proceedings of the Physiological Society. University College London Meeting, 1964. 172 (Suppl), 19P-21P.

Bönisch, H., Bryan, L. J., Henseling, M., O'Donnell, S. R., Stockmann, P. & Trendelenburg, U. (1985) The effect of various ions on uptake$_2$ of catecholamines. *Naunyn Schmiedebergs Arch Pharmacol,* **328,** 407-16.

Brain, K. L. & Bennett, M. R. (1997) Calcium in sympathetic varicosities of mouse vas deferens during facilitation, augmentation and autoinhibition. *J Physiol,* **502 (Pt 3),** 521-36.

Brain, K. L., Jackson, V. M., Trout, S. J. & Cunnane, T. C. (2002) Intermittent ATP release from nerve terminals elicits focal smooth muscle Ca^{2+} transients in mouse vas deferens. *J Physiol,* **541,** 849-62.

Brosenitsch, T. A. & Katz, D. M. (2001) Physiological patterns of electrical stimulation can induce neuronal gene expression by activating N-type calcium channels. *J Neurosci,* **21,** 2571-9.

Burnstock, G. (2013) Cotransmission in the autonomic nervous system. *Handb Clin Neurol,* **117,** 23-35.

Callado, L. F. & Stamford, J. A. (2000) Spatiotemporal interaction of α_2 autoreceptors and noradrenaline transporters in the rat locus coeruleus. *J Neurochem,* **74,** 2350-58.

Cao, L. L., Holmes, A. P., Marshall, J. M., Fabritz, L. & Brain, K. L. (2020) Dynamic monitoring of single-terminal norepinephrine transporter rate in the rodent cardiovascular system: A novel fluorescence imaging method. *Auton Neurosci,* **223,** 102611.

Cervoni, P. & Kirpekar, S. M. (1966) Studies on the decentralized nictitating membrane of the cat. I. Effect of postganglionic electrical stimulation on the response to exogenous catecholamines. *J Pharmacol Exp Ther,* **152,** 8-17.

Chang, C. C. & Chiueh, C. C. (1969) Modulation of noradrenaline incorporation by nerve activities in the rat submaxillary gland. *J Physiol,* **203,** 145-57.

Esler, M., Jennings, G., Lambert, G., Meredith, I., Horne, M. & Eisenhofer, G. (1990) Overflow of catecholamine neurotransmitters to the circulation: source, fate, and functions. *Physiol Rev,* **70,** 963-85.

Gibbins, I. L. (1991) Vasomotor, pilomotor and secretomotor neurons distinguished by size and neuropeptide content in superior cervical ganglia of mice. *J Auton Nerv Syst,* **34,** 171-83.

Gillis, C. N. (1963) Increased retention of exogenous norepinephrine by cat atria after electrical stimulation of the cardioaccelerator nerves. *Biochem Pharmacol,* **12,** 593-5.

Gilsbach, R. & Hein, L. (2012) Are the pharmacology and physiology of α_2 adrenoceptors determined by α_2-heteroreceptors and autoreceptors respectively? *Br J Pharmacol,* **165,** 90-102.

Goldstein, D. S., Brush, J. E., Jr., Eisenhofer, G., Stull, R. & Esler, M. (1988) In vivo measurement of neuronal uptake of norepinephrine in the human heart. *Circulation,* **78,** 41-8.

Gonon, F., Bao, J. X., Msghina, M., Suaud-Chagny, M. F. & Stjärne, L. (1993) Fast and local electrochemical monitoring of noradrenaline release from sympathetic terminals in isolated rat tail srtery. *J Neurochem,* **60,** 1251-57.

Habecker, B. A., Willison, B. D., Shi, X. & Woodward, W. R. (2006) Chronic depolarization stimulates norepinephrine transporter expression via catecholamines. *J Neurochem,* **97,** 1044-51.

Häbler, H. J., Jänig, W., Krummel, M. & Peters, O. A. (1994) Reflex patterns in postganglionic neurons supplying skin and skeletal muscle of the rat hindlimb. *J Neurophysiol,* **72,** 2222-36.

Häggendal, J. & Malmfors, T. (1969) The effect of nerve stimulation on the uptake of noradrenaline into the adrenergic nerve terminals. *Acta Physiol Scand,* **75,** 28-32.

Iversen, L. L. (1963) The uptake of noradrenaline by the isolated perfused rat heart *Br J Pharmacol Chemother,* **21,** 523-37.

Iversen, L. L. (1965) The uptake of catechol amines at high perfusion concentrations in the rat isolated heart: A novel catechol amine uptake process. *Br J Pharmacol,* **25,** 18-33.

Kaludercic, N., Takimoto, E., Nagayama, T., Feng, N., Lai, E. W., Bedja, D., . . . Paolocci, N. (2010) Monoamine oxidase A-mediated enhanced catabolism of norepinephrine contributes to adverse remodeling and pump failure in hearts with pressure overload. *Circ Res,* **106,** 193-202.

Kazanietz, M. G. & Enero, M. A. (1989) Modulation of noradrenaline release by presynaptic alpha$_2$ and β adrenoceptors in rat atria. Effect of pretreatment with clenbuter. *Naunyn Schmiedebergs Arch Pharmacol,* **340,** 274-8.

Kirpekar, S. M. & Wakade, A. R. (1968) Factors influencing noradrenaline uptake by the perfused spleen of the cat. *J Physiol,* **194,** 609-26.

Li, C. & Horn, J. P. (2008) Differential inhibition of Ca^{2+} channels by α_2-adrenoceptors in three functional subclasses of rat sympathetic neurons. *J Neurophysiol,* **100,** 3055-63.

Liang, C. S., Fan, T. H., Sullebarger, J. T. & Sakamoto, S. (1989) Decreased adrenergic neuronal uptake activity in experimental right heart failure. A chamber-specific contributor to beta-adrenoceptor downregulation. *J Clin Invest,* **84,** 1267-75.

Major, H., Sauerwein, I. & Graefe, K. H. (1978) Kinetics of the uptake and metabolism of ^{3}H-(±) isoprenaline in the rat submaxillary gland. *Naunyn Schmiedebergs Arch Pharmacol,* **305,** 51-63.

Mandela, P. & Ordway, G. A. (2006a) KCl stimulation increases norepinephrine transporter function in PC12 cells. *J Neurochem,* **98,** 1521-30.

Mandela, P. & Ordway, G. A. (2006b) The norepinephrine transporter and its regulation. *J Neurochem,* **97,** 310-33.

Nilsson, H., Ljung, B., Sjöblom, N. & Wallin, B. G. (1985) The influence of the sympathetic impulse pattern on contractile responses of rat mesenteric arteries and veins. *Acta Physiol Scand,* **123,** 303-09.

Nishimaru, K., Tanaka, Y., Tanaka, H. & Shigenobu, K. (2000) Positive and negative inotropic effects of muscarinic receptor stimulation in mouse left atria. *Life Sci,* **66,** 607-15.

Oostendorp, J. & Kaumann, A. J. (2000) Pertussis toxin suppresses carbachol-evoked cardiodepression but does not modify cardiostimulation mediated through β_1-

and putative β_4-adrenoceptors in mouse left atria: no evidence for β_2- and β_3-adrenoreceptor function. *Naunyn Schmiedebergs Arch Pharmacol,* **361,** 134-45.

Palaić, D. & Panisset, J.-C. (1969) Effect of nerve stimulation and angiotensin on the accumulation of ^{3}H-norepinephrine and the endogenous norepinephrine level in guinea pig vas deferens. *Biochem Pharmacol,* **18,** 2693-700.

Parker, L. K., Shanks, J. A., Kennard, J. A. & Brain, K. L. (2010) Dynamic monitoring of NET activity in mature murine sympathetic terminals using a fluorescent substrate. *Br J Pharmacol,* **159,** 797-807.

Regehr, W. G., Carey, M. R. & Best, A. R. (2009) Activity-dependent regulation of synapses by retrograde messengers. *Neuron,* **63,** 154-70.

Reilly, J. P. & Diamant, A. M. (2011) Chapter 6: Model application to C-fibers and the heart. *In:* REILLY, J. P. & DIAMANT, A. M. *Electrostimulation: theroy, applications and computational model.* Artech House Publishers.

Rook, W., Johnson, C. D., Coney, A. M. & Marshall, J. M. (2014) Prenatal hypoxia leads to increased muscle sympathetic nerve activity, sympathetic hyperinnervation, premature blunting of neuropeptide Y signaling, and hypertension in adult life. *Hypertension,* **64,** 1321-7.

Savchenko, V., Sung, U. & Blakely, R. D. (2003) Cell surface trafficking of the antidepressant-sensitive norepinephrine transporter revealed with an ectodomain antibody. *Mol Cell Neurosci,* **24,** 1131-50.

Schroeder, C. & Jordan, J. (2012) Norepinephrine transporter function and human cardiovascular disease. *Am J Physiol Heart Circ Physiol,* **303,** H1273-82.

Shanks, J., Mane, S., Ryan, R. & Paterson, D. J. (2013a) Ganglion-specific impairment of the norepinephrine transporter in the hypertensive rat. *Hypertension,* **61,** 187-93.

Shanks, J., Manou-Stathopoulou, S., Lu, C. J., Li, D., Paterson, D. J. & Herring, N. (2013b) Cardiac sympathetic dysfunction in the prehypertensive spontaneously hypertensive rat. *Am J Physiol Heart Circ Physiol,* **305,** H980-6.

Shivkumar, K. & Ardell, J. L. (2016) Cardiac autonomic control in health and disease. *J Physiol,* **594,** 3851-2.

Starke, K. (2001) Presynaptic autoreceptors in the third decade: focus on α_2-adrenoceptors. *J Neurochem,* **78,** 685-93.

Stjärne, L. (1989) Basic mechanisms and local modulation of nerve impulse-induced secretion of neurotransmitters from individual sympathetic nerve varicosities. *Reviews of Physiology, Biochemistry and Pharmacology.* Berlin, Heidelberg: Springer Berlin Heidelberg.

Stjärne, L., Bao, J. X., Gonon, F. & Msghina, M. (1994) Nerve activity-dependent variations in clearance of released noradrenaline: Regulatory roles for sympathetic neuromuscular transmission in rat tail artery. *Neuroscience,* **60,** 1021-38.

Stjärne, L., Bao, J. X., Gonon, F., Msghina, M. & Stjärne, E. (1993) A nonstochastic string model of sympathetic neuromuscular transmission. *News Physiol Sci,* **8,** 253-60.

Stjärne, L. & Stjärne, E. (1995) Geometry, kinetics and plasticity of release and clearance of ATP and noradrenaline as sympathetic cotransmitters: roles for the neurogenic contraction. *Prog Neurobiol,* **47,** 45-94.

Struik, R. J. (2017) Stimulation and recording *In:* HORCH, K. & KIPKE, D. *Neuroprosthetics: theory and practise.* Second ed. Singapore World Scientific Co.

Sung, U., Binda, F., Savchenko, V., Owens, W. A. & Daws, L. C. (2017) Ca^{2+} dependent surface trafficking of norepinephrine transporters depends on threonine 30 and Ca^{2+} calmodulin kinases. *J Chem Neuroanat,* **83-84,** 19-35.

Trendelenburg, A.-U., Gomeza, J., Klebroff, W., Zhou, H. & Wess, J. (2003) Heterogeneity of presynaptic muscarinic receptors mediating inhibition of sympathetic transmitter release: a study with M_2- and M_4-receptor-deficient mice. *Br J Pharmacol,* **138,** 469-80.

Ungerer, M., Chlistalla, A. & Richardt, G. (1996) Upregulation of cardiac uptake$_1$ carrier in ischemic and nonischemic rat heart. *Circ Res,* **78,** 1037-43.

Wehrwein, E. A., Orer, H. S. & Barman, S. M. (2016) Overview of the anatomy, physiology, and pharmacology of the autonomic nervous system. *Compr Physiol,* **6,** 1239-78.

Weinshenker, D. & Schroeder, J. P. (2007) There and back again: a tale of norepinephrine and drug addiction. *Neuropsychopharmacology,* **32,** 1433-51.

Yamamoto, H. & Kirpekar, S. M. (1972) Effects of nerve stimulation on the uptake of norepinephrine by the perfused spleen of the cat. *Eur J Pharmacol,* **17,** 25-33.

Yang, Q., Sumner, A. D., Puhl, H. L. & Ruiz-Velasco, V. (2006) M_1 and M_2 muscarinic acetylcholine receptor subtypes mediate Ca^{2+} channel current inhibition in rat sympathetic stellate ganglion neurons. *J Neurophysiol,* **96,** 2479-87.

Zhou, J. (2004) Norepinephrine transporter inhibitors and their therapeutic potential. *Drugs Future,* **29,** 1235-44.

Zugck, C., Lossnitzer, D., Backs, J., Kristen, A., Kinscherf, R. & Haass, M. (2003) Increased cardiac norepinephrine release in spontaneously hypertensive rats: role of presynaptic alpha-2_A adrenoceptors. *J Hypertens,* **21,** 1363-9.